

Investigation Of Spectroscopic And Electronic Properties Of Some Schiff Bases derived From 2-Hydroxy-3-Methoxy-5-Nitrobenzaldehyde By Dft Method

ASEEL ETHAR SAADALLAH SAADALLAH

Department of Physics
Çankırı Karatekin University
TURKEY

HAMİT ALYAR

Department of Physics
Çankırı Karatekin University
TURKEY

SALIHA ALYAR

Department of CHEMISTRY
Çankırı Karatekin University
TURKEY

Abstract: - In this study, the theoretical spectroscopic and some electronic properties of MMP and FMP compounds were investigated and the obtained theoretical results were compared with some experimental values. For this purpose, firstly, MMP and FMP compounds were optimized by DFT method using the B3LYP functional and the 6-311G++(d,p) basis set. With the help of the optimized structure obtained, the chemical shift values of H-NMR and ¹³C-NMR were calculated in the gas phase by the Gaussian G09 (Linux) and Gauss View 5.0 programs according to the GIAO method. According to the results obtained, it was seen that the theoretical values were compatible with the experimental values. In the theoretical part of the study, the IR frequency values of the studied compounds were calculated using the same method and basis set, and vibration frequencies were marked. Finally, the nonlinear optical properties of the compounds of interest; Polarizability and hyperpolarizability values were calculated by making polar calculations in the single point energy calculation. As a result of the calculations, the energy band gaps between the HOMO and LUMO orbitals of MMP and FMP are 1.34 eV and 3.64 eV. First static hyperpolarizability of MMP and FMP were found as 29273.7 x 10⁻³³ and 26500.5 x 10⁻³³ esu, respectively.

Key-Words: - FT-IR, NMR, NLO, DFT, HOMO- LUMO

Received: June 8, 2022. Revised: August 13, 2023. Accepted: September 15, 2023. Published: October 6, 2023.

1 Introduction

Schiff bases (Figure 1.1), first synthesized by the Nobel Prize-winning German chemist Hugo Schiff in 1864, are compounds containing carbon nitrogen double bonds (-CH=N) and obtained as a result of the nucleophilic addition reaction of aldehydes or ketones with amines [1]. The bond formed as a result of the reaction with aldehyde is known as azomethine or aldimine. The bond formed as a result of its reaction with ketone is called imine or ketimine. Schiff bases (imines) have become one of the compounds of interest because they are stable and easily synthesized. This interest in imines can be

explained by their use in many biological systems [2], chemical catalysis [3], medicine and pharmacy [4], chemical analysis, and new technologies [5,6].

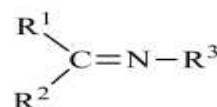


Figure 1. General representation of Schiff bases (R₁, R₂, R₃ = aryl or alkyl)

The importance of coordination compounds in both biological systems and industry is increasing day by day. Schiff bases are among the ligands widely used in coordination

chemistry due to their structural and biological properties. Its use as a ligand was first described by Pfeiffer et al. [7], Metal complexes of Schiff bases reported by Schiff are studied with interest [8].

With the theoretical calculation methods used today, many properties of molecules do not require experimental analysis, can be examined. In some studies, more sensitive and reliable results can be obtained than the experimental method. There is no method that can give a lot of information such as molecular structure, formation temperature, dipole moment, ionization potential, electron charges, electron densities, bond lengths with a single experiment. Considering the reliability of the results in the calculation of such data with the experimental method, it can be seen how reliable the results of many calculation methods, which are becoming common, are compared to the experimental results.

In this study, the structure of two Schiff bases was tried to be elucidated theoretically by using spectroscopic methods such as FT-IR, ¹H-NMR and ¹³C-NMR. The NMR study was performed using the GIAO method in DMSO solution. After these studies, the HOMO-LUMO molecular orbital energies, nonlinear optical properties and potential energy surfaces of these Schiff base compounds were calculated using the DFT/B3LYP method and the 6-311++G(d,p) basis set.

2 Materials and Methods

First of all, the structure of 2-((2,4-Dimethylphenylimino)methyl)-6-methoxy-4-nitrophenol (MPM) and 2-((3,4-Difluorophenylimino)methyl)-6-methoxy-4-nitrophenol (FPM) compounds synthesized by Joshi *et al.* [9] for the first time we will optimize with DFT/B3LYP/6-311++G (d, p) theoretical level and lowest energy stable structures will be obtained. Then, the vibration frequencies of these compounds, ¹H and ¹³C NMR calculations will be made with the same basis set in the DMSO phase and compared with the experimental data. Finally, HOMO and LUMO molecular orbital energies, nonlinear optical properties (NLO) and molecular electrostatic

potential (MESP) maps will be examined at the DFT/B3LYP/6-311++G (d, p) theory level. The theoretical results obtained from the calculations will be interpreted by comparing them with the existing experimental values. All calculations will be performed with Gaussian 09 [10] and Gauss View 5.0 package programs.

3 Results and Discussion

3.1 Geometrical Optimization of compounds

The three-dimensional approximate geometry of the 2-((2,4-Dimethylphenylimino) methyl)-6-methoxy-4-nitrophenol (MPM) and 2-((3,4-Difluorophenylimino) methyl)-6-methoxy-4-nitrophenol (FPM) compounds were drawn in the GaussView 5.0 program [11]. Geometry optimizations of 2-((2,4-Dimethylphenylimino) methyl)-6-methoxy-4-nitrophenol (MPM) and 2-((3,4-Difluorophenylimino)methyl)-6-methoxy-4-nitrophenol (FPM) were achieved by selecting 6-311G ++ (d, p) base set in the "Gaussian 09" program, using density functional theory (DFT) method.

As a result of the calculations, the ground state energies of 2-((2,4-Dimethylphenylimino) methyl)-6-methoxy-4-nitrophenol (MPM) and 2-((3,4-Difluorophenylimino) methyl)-6-methoxy-4-nitrophenol (FPM) were found as -1029.74 a.u and -1149.79 a.u, respectively. By using the optimized structures, the bond lengths and bond angles of the molecules were calculated theoretically. Stable structures of MPM and FPM are shown in Figure 4.1 and Figure 4.2. X-ray crystal data of the MPM and FPM molecules could not be found in the literature. In the literature, all C-H bond lengths in the benzene ring have been measured as approximately 1.084 Å, and C-C bond lengths as 1.397 Å. In this study, the aromatic C-H values of MPM compound were calculated as 1.084, 1.085 and 1.086 Å for C₃-H₇, C₄-H₈ and C₆-H₉, respectively. Also, the average values of aromatic C-C bond lengths for MPM compound were calculated as 1.398 Å.

In addition, one of the most important bonds in the studied molecules is the imine bond(C=N). The experimental values of the C=N bond lengths (1E,2E)-phenyl-[(1-phenylethyl) imino]-ethanal oxime were measured as 1,280 Å and 1,275 Å, respectively [12]. Theoretical values were calculated as 1,280 Å and 1,276 Å, respectively [12].

In this study, the C=N imine bond for MMP and FMP compounds was calculated as 1.287Å and 1.275 Å, respectively. These results are in good agreement with previous experimental and theoretical data. C-N bond length of 2- (2- (3-Nitrofenil) hidrazono) -5,5- dimetilsikloheksan -1, 3- dion compound was measured 1.411 Å and calculated as 1.405 Å [13].

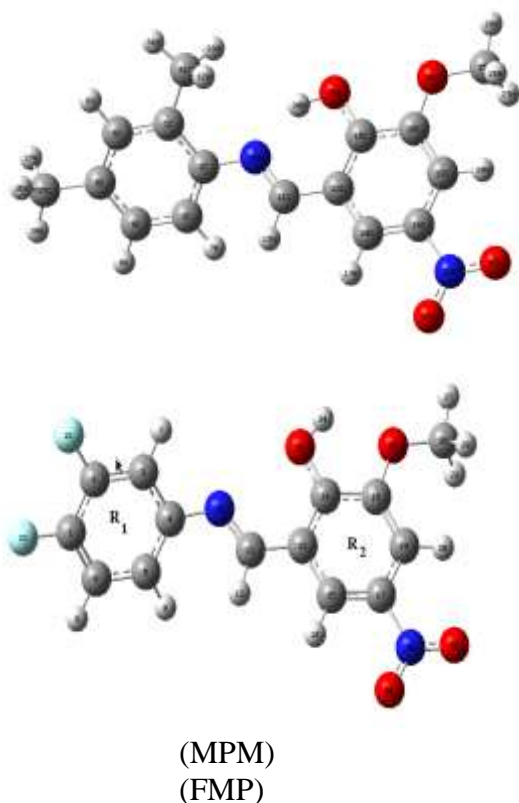


Figure 3.1 Optimized structures of MPM and FMP compounds

3.2 Vibrational Assignment of MPM and FMP compounds

The CH stretching vibration is expected in the 3000–3200 cm^{-1} range [15]. Two bands of moderate intensity observed at 3049–3060 and

The vibration spectrum (IR) of 2-((2,4-Dimethylphenylimino) methyl)-6-methoxy-4-nitrophenol (MPM) and 2-((3,4-Difluorophenylimino) methyl)-6-methoxy-4-nitrophenol (FPM) molecules have been experimentally investigated in the middle IR region of 4000-500 cm^{-1} before [9]. However, it is known that there are no theoretical results for these molecules in the literature. In this study, calculations were made using the DFT/B3LYP/6-311++G(d,p) method theoretically in the same region to compare with the experimental results. These calculations are important for understanding the vibration spectrum and molecular parameters.

When the obtained results (theoretical and experimental) were compared, it was observed that they were in agreement with the results in the literature. It was observed that there were very small differences between the experimental results and the theoretical results. The reason for this can be explained as follows: the experimentally obtained IR spectra of molecules are the spectrum of all IR interactions that the spectrometer can see when the sample is in solid or liquid state. But theoretical wave numbers are the values obtained by using fundamental sets made with a purely quantum mechanical approach. Due to the limitations of these sets, there are differences between the experimental results and the theoretical results.

The OH stretching vibration is generally observed in the range of 3600 to 3400 cm^{-1} . Also, this band appears as a very broad band in the FT-IR spectrum. OH vibration bands show intramolecular and intermolecular hydrogen bonding [14]. Joshi et al. [9] observed the IR spectra of MPM and FPM ligands as a wide band in the range of 3420-3460 cm^{-1} due to stretching vibrations of the phenolic hydroxyl group [9]. In this study, OH stretching vibrations were observed at 3449 and 3442 cm^{-1} and calculated at 3455 and 3727 cm^{-1} .

2985–3005 cm^{-1} are due to aromatic and aliphatic $\nu(\text{C-H})$, respectively [9]. These

vibrations calculated at 3044-3027 cm^{-1} and 3202-3188 cm^{-1} for MPM and FPM compounds.

The vibration frequencies of the azomethine group (C=N) were experimentally observed at

1614 cm^{-1} . This stretching vibration was calculated as 1671, 1636 and 1624 cm^{-1} for the MMP compound and as 1694 and 1638 cm^{-1} for the FPM compound.

Table 3.1 Vibrational assignment of 2-((2,4-Dimethylphenylimino) methyl)-6-methoxy-4-nitrophenol (MPM) compound using B3LYP/6-311++G (d, p) level of theory

Mode	Exp. [9]	Intensity	Calculation	Assignment
108	3449	10.61	3455	v(O24H25)
107		8.06	3324	v(C22H31)
106	3105	14.51	3322.77	vS (C27H3)
105		10.69	3318.10	vas (C35H3)
104		14.19	3315.09	vas (C10H3)
103		15.01	3309.77	vas (C35H3)
101		18.96	3304.29	vas (C27H3)
100		10.60	3303.10	v (C15H16)
99		18.24	3222.47	vs (C35H3)
98		34.17	3220.37	vs (C10H3)
97		29.43	3218.70	vs (C27H3)
96	3003	11.47	3044.61	vs (CH)ring1
95	2900	15.57	3033.39	vs (C2H)
94		11.62	3029	v (C20H)
93		10.37	3027.01	vas (CH)ring1
92		84.52	1785.24	v (CC)ring2
91		60.30	1671.26	v (C=N) + v (CC)ring2+ β (C20H)
90		5.43	1636.28	v (C=N) + v (CC)ring1+ β (CCH)ring1
89	1614	0.53	1624.13	v (C=N) + v (CC)ring1+ β (CCH)ring1
88		54.03	1580.62	v (CC)ring2+ β (CCH)ring2 + β (C27H3)
87	1549	4.44	1570.07	v (CC)ring2+ β (CCH)ring2 + β (C27H3)
86		30.84	1531.27	β (C27H3)
85	1483	28.93	1515.48	v (CC)ring1+ β (CCH)ring1
84		13.61	1477.68	β (C27H3)
83		18.81	1473.80	v (CC)ring1+ β (CCH)ring1 + β (C10H3)
82		2.82	1461.48	β (C10H3) + β (C35H3)
81		10.72	1456.98	β (C10H3)
80		4.15	1451.79	β (C35H3)
79		9.84	1445.81	γ (C27H3)
78		0.70	1424.35	v (CC)ring1+ β (CCH)ring1 + β (C10H3) + β (C35H3)
77		11.96	1398.25	v (CC)ring2+ β (CCH)ring2 + β (C18OH)
76		0.78	1338.40	v (CC)ring1+ γ (C10H3) + γ (C35H3)
75	1330	3.02	1334.11	γ (C35H3)
74		1.78	1327.33	γ (C10H3)
73		9.61	1309.37	v (CC)ring1+ β (CCH)ring1
72		25.31	1305.91	v (CC)ring2+ β (CCH)ring2
71	1280	51.27	1260.94	v (C23O)+v (CC)ring2+ β (CCH)ring2 + β (C18OH)
70		35.82	1230.79	β (C15H)
69		2.41	1226.23	v (C3C10)+v (CC)ring1+ β (CCH)ring1+ β (N14CH)

68	1209	152.23	1188.83	ν (CC)ring2+ β (CCH)ring2+ β (C18OH) + γ (C27H3)
67		28.26	1177.73	ν (C1C35)+ ν (C6N) + ν (CC)ring1+ β (CCH)ring1
66		4.19	1172.42	ν (C1C35)+ ν (C6N) + ν (CC)ring1+ β (CCH)ring1
65		38.20	1163.18	γ (C27H3) + β (C18OH)
64		9.11	1129.28	γ (C27H3)

Table 3.1 (Continued)

63		12.11	1121.27	ν (CC)ring2+ β (CCH)ring2+ β (C18OH) + γ (C27H3)
62	1101	120.74	1097.73	ν (C6N)+ ν (C18O)+ β (CCC)ring1+ β (CCC)ring2
61		18.66	1093.19	ν (C6N)+ ν (C18O)+ β (CCC)ring1+ β (CCC)ring2
60		164.93	1053.05	ν (C27O)
59		7.75	1019.27	γ (C35H3)+ γ (C10H3)
58		0.94	1014.36	γ (C35H3) + γ (C10H3) + γ (CH)ring1
57		6.73	995.14	γ (C35H3) + γ (C10H3) + γ (CH)ring1
55		7.43	947.29	γ (C35H3) + γ (C10H3)
54		201.52	986.24	ν (C17C15)+ ν (C19N)+ β (CCC)ring2
53		3.21	940.09	γ (C35H3) + γ (C10H3)
52		51.87	933.93	ν (C19N)+ β (C17C15N) + γ (C22H)
51		1.16	919.62	γ (CH)ring1
50		4.73	912.88	ν (C1C35) + ν (C3C10) + β (CCC)ring1
49		4.77	897.64	ν (C15N) + γ (C22H)
48	886	44.25	877.32	ν (C15N) + γ (CH)ring1
47		77.08	858.51	ν (C23O) + ν (C18O) + ν (N32O) + β (CCC)ring2
46		98.52	838.62	ν as (NO2) + γ (C15H)
45		16.93	834.80	ν (C15N) + γ (C15H)+ τ (CCCH)ring1+ τ (CCCC)ring2
44		6.48	813.25	ν (C15N) + γ (CH)ring1
43	819	126.37	804.72	ν as (NO2) + ν (C5N) + β (CCC)ring1+ β (CCC)ring2
42	751	134.89	748.90	ν s (NO2) + ν (C18O) + β (CCC)ring1
41		7.03	731.32	τ (CCCH)ring1+ τ (CCCC)ring1+ τ (CCCH)ring2+ τ (CCCC)ring2 + τ (CCCO)ring2
40		7.06	726.87	ν (C1C35) + β (CCC)ring1+ β (CCC)ring2+ β (NO2)
39		8.71	717.22	β (NO2)+ τ (CCCH)ring + τ (CCCC)ring
38		1.44	706.33	ν (C6N) + τ (CCCH)ring + τ (CCCC)ring + τ (CCCO)ring
37		16.36	650.03	τ (N32CCH)+ τ (CC-NO2)+ τ (N32CCC)
36		31.74	629.17	β (CCC)ring2+ β (CCO24)+ τ (CCCN14)
35		5.01	610.39	β (CCO24) + τ (CCCN14)
34		5.88	578.16	τ (CCCH)ring + τ (CCCC)ring + τ (CCCO)ring
33		19.54	565.82	τ (CCCH)ring2+ τ (CCCC)ring2 + τ (CCCO)ring2+ τ (N32CCC) + τ (N32CCH)
32		9.56	546.22	β (CCC)ring1

Table 3.2 Vibrational assignment of 2-((3,4-Difluorophenylimino) methyl)-6- methoxy-4-nitrophenol (FPM) compound using B3LYP/6-311++G (d, p) level of theory

Mode	Exp.[9]	Calculation	Intensity	Assignment
90	3442	3727	175.89	ν (O ₂₃ H ₂₅)
89		3238	10.66	ν (C ₁₉ H)
87		3210	1.11	ν (C3H)
86	3049	3202	1.14	ν _s (CH) _{ring}
85	2985	3188	4.13	ν _{as} (CH) _{ring}
84		3150	12.64	ν _{as} (C26H ₃)
83		3090	22.45	ν _{as} (C26H ₃)
82		3023	42.45	ν _s (C26H ₃)

81		2998	32.99	$\nu(\text{C11H})$
80	1614	1694	91.90	$\nu(\text{C=N})$
79		1655	49.76	$\nu(\text{CC})_{\text{ring}} + \nu_{\text{as}}(\text{NO}_2) + \nu(\text{C11C13}) + \beta(\text{C14OH})$
78		1638	71.43	$\nu(\text{CC})_{\text{ring}} + \nu(\text{C=N}) + \beta(\text{CCH})_{\text{ring1,2}}$
77		1626	68.50	$\nu(\text{CC})_{\text{ring1}}$
76		1618	3.75	$\nu(\text{CC})_{\text{ring2}} + \beta(\text{CCH})_{\text{ring2}}$
75	1498	1576	251.10	$\nu_{\text{as}}(\text{NO}_2) + \beta(\text{C14OH})$
74		1534	322.50	$\nu(\text{CC})_{\text{ring1}} + \beta(\text{CCH})_{\text{ring1}}$
73		1513	108.93	$\nu(\text{CC})_{\text{ring2}} + \beta(\text{C26H}_3)$
72		1502	148.40	$\beta(\text{C26H}_3)$
71		1493	12.02	$\beta(\text{C26H}_3)$
70		1487	9.4	$\gamma(\text{C26H}_3)$
69		1470	47.33	$\nu(\text{CC})_{\text{ring1,2}} + \beta(\text{CCH})_{\text{ring1,2}} + \beta(\text{NCH}) + \gamma(\text{C26H}_3)$
68		1450	27.50	$\nu(\text{CC})_{\text{ring1,2}} + \beta(\text{CCH})_{\text{ring1,2}} + \beta(\text{NCH}) + \gamma(\text{C26H}_3)$
67		1426	29.35	$\nu(\text{CC})_{\text{ring1}} + \beta(\text{CCH})_{\text{ring1}} + \beta(\text{C14OH}) + \gamma(\text{C26H}_3)$
66		1405	61.24	$\nu(\text{CC})_{\text{ring1}} + \beta(\text{CCH})_{\text{ring1}} + \beta(\text{C14OH}) + \gamma(\text{C26H}_3)$
65	1329	1356	603.23	$\nu(\text{C17N})$
64		1328	9.31	$\nu(\text{CC})_{\text{ring1,2}} + \nu(\text{C11C13}) + \beta(\text{C14OH})$
63		1318	38.38	$\nu(\text{CC})_{\text{ring1,2}} + \nu(\text{C11C13}) + \beta(\text{C14OH})$
62		1303	120.03	$\nu(\text{CC})_{\text{ring2}} + \nu(\text{C4N}) + \beta(\text{C14OH})$
61		1301	165.78	$\nu(\text{CC})_{\text{ring1}} + \nu(\text{C14O}) + \beta(\text{C19H})$
60		1282	62.65	$\nu(\text{CC})_{\text{ring1,2}} + \nu(\text{C16O}) + \beta(\text{CCH})_{\text{ring1}}$
59		1274	168.41	$\nu(\text{CC})_{\text{ring1,2}} + \nu(\text{C16O}) + \beta(\text{CCH})_{\text{ring1}}$
58		1226	59.63	$\nu(\text{CC})_{\text{ring1,2}} + \nu(\text{C16O}) + \beta(\text{CCH})_{\text{ring1,2}}$
57		1216	35.39	$\nu(\text{CC})_{\text{ring1,2}} + \nu(\text{C1F}) + \nu(\text{C2F}) + \beta(\text{CCH})_{\text{ring1,2}}$
56	1204	1206	10.53	$\beta(\text{CCH})_{\text{ring1,2}} + \beta(\text{C26H}_3)$
55		1170	0.67	$\beta(\text{C26H}_3)$
54		1160	55.78	$\nu(\text{CC})_{\text{ring1}} + \nu(\text{C4N}) + \beta(\text{CCH})_{\text{ring1}}$
53	1147	1127	64.16	$\nu(\text{C26O}) + \nu(\text{CC})_{\text{ring1,2}} + \beta(\text{CCH})_{\text{ring1}}$
52		1120	64.69	$\nu(\text{C4N}) + \nu(\text{C26O}) + \nu(\text{C2F}) + \beta(\text{CCH})_{\text{ring1}}$
51	1098	1111	124.40	$\nu(\text{CC})_{\text{ring2}} + \nu(\text{C17N}) + \beta(\text{CCH})_{\text{ring2}}$
50		1002	7.59	$\gamma(\text{C11H})$

Table 3.2 (Continued)

49		984	50.49	$\nu(\text{C11C13}) + \nu(\text{C17N}) + \beta(\text{CCC})_{\text{ring2}}$
48	970	971	67.84	$\nu(\text{CC})_{\text{ring1}} + \nu(\text{C4N})$
47		947	5.19	$\gamma(\text{CH})_{\text{ring1}}$
46		946	0.96	$\nu(\text{C26O}) + \nu(\text{C17N}) + \gamma(\text{CH})_{\text{ring1}}$
45		916	1121.27	$\gamma(\text{C15H}) + \gamma(\text{C11H})$
44		891	27.82	$\gamma(\text{C3H})$
43		886	26.95	$\gamma(\text{C19H})$
42	870	836	25.99	$\nu(\text{C14O}) + \beta(\text{CCC})_{\text{ring1,2}} + \beta(\text{NO}_2)$
41	819	828	20.02	$\gamma(\text{CH})_{\text{ring1}}$
40		802	61.10	$\beta(\text{CCN10}) + \beta(\text{CCC})_{\text{ring1,2}} + \tau(\text{CH})_{\text{ring1}}$
39		786	40.13	$\nu(\text{CC})_{\text{ring1,2}} + \beta(\text{CCC})_{\text{ring1,2}} + \text{sci}(\text{NO}_2)$
38		768	16.39	$\nu(\text{CC})_{\text{ring1,2}} + \beta(\text{CCC})_{\text{ring1,2}}$
37	747	757	1.05	$\tau(\text{CCCH})_{\text{ring1,2}} + \tau(\text{CCCC})_{\text{ring1,2}} + \tau(\text{CCCO23}) + \tau(\text{CCCO25}) + \tau(\text{CCCN30}) + \tau(\text{CCCN10})$
36		720	17.14	$\tau(\text{CCCH})_{\text{ring2}} + \tau(\text{CCCC})_{\text{ring2}} + \tau(\text{CCCO23}) + \tau(\text{CCCO25}) + \tau(\text{CCCN30}) + \tau(\text{CC-NO}_2)$

35		711.39	1.88	$\tau(\text{CCCH})_{\text{ring1}} + \tau(\text{CCCC})_{\text{ring1}} + \tau(\text{CCCF22}) + \tau(\text{CCCF21}) + \tau(\text{CCCN10})$
34		687	15.23	$\beta(\text{CCC})_{\text{ring1,2}} + \beta(\text{C4NC11}) + \beta(\text{C13C11N10})$
33		656	6.66	$\beta(\text{C13C11C15}) + \tau(\text{CCCH})_{\text{ring1}} + \tau(\text{CCCC})_{\text{ring1}} + \tau(\text{CCCF22}) + \tau(\text{CCCF21}) + \tau(\text{CCCN10})$
32	617	621	1.80	$\beta(\text{C13C11C15}) + \tau(\text{CCCH})_{\text{ring1}} + \tau(\text{CCCC})_{\text{ring1}} + \tau(\text{CCCF22}) + \tau(\text{CCCF21}) + \tau(\text{CCCN10})$
31		592	3.54	$\beta(\text{C3C4N10}) + \beta(\text{C5C4N10}) + \tau(\text{CCCH})_{\text{ring2}} + \tau(\text{CCCC})_{\text{ring2}} + \tau(\text{CCCO23}) + \tau(\text{CCCO25})$
30		573	10.99	$\beta(\text{CCC})_{\text{ring1}} + \tau(\text{CCCH})_{\text{ring2}} + \tau(\text{CCCC})_{\text{ring2}} + \tau(\text{CCCO23}) + \tau(\text{CCCO25}) + \tau(\text{CCO23H})$
29		552	15.38	$\beta(\text{CCC})_{\text{ring1}} + \tau(\text{CCCH})_{\text{ring2}} + \tau(\text{CCCC})_{\text{ring2}} + \tau(\text{CCCO23}) + \tau(\text{CCCO25}) + \tau(\text{CCO23H})$
28		544	68.11	$\tau(\text{CCCH})_{\text{ring2}} + \tau(\text{CCCC})_{\text{ring2}} + \tau(\text{CCCO23})$
27	499	527	14.89	$\tau(\text{CCCH})_{\text{ring2}} + \tau(\text{CCCC})_{\text{ring2}} + \tau(\text{CCCO23}) + \tau(\text{CC-NO}_2)$

3.3 NMR Results of MPM and FPM Molecules

NMR spectroscopy is one of the important techniques used in the determination of the structure analysis of organic compounds. It is carried out using the ^1H and ^{13}C NMR chemical shift values. The measurements of the ^1H and ^{13}C NMR chemical shift values of the molecules

were taken in DMSO. The ^1H and ^{13}C NMR chemical shift values of the MPM and FPM molecules were calculated over the optimized molecular structures, using the Gauge-Independent Atomic Orbital (GIAO) method [16,17]. Theoretical calculations were performed in DMSO solution with the DFT/B3LYP method and 6-311G++(d,p) base set. NMR results were tabulated at Table 3.3.

Table 3.3 ^1H -NMR and ^{13}C -NMR Results of MMP and FMP compounds

Assignment	(MPM)		Assignment	(FPM)	
	□ exp. [9]	□ calc.		□ calc.	
C15	-	221.1001	C11		138.388
C19	-	179.2248	C14		143.259
C6	-	155.2287	C2		133.793
C18	-	152.9903	C4		132.387
C23	-	144.0097	C16		128.856
C3	-	139.9785	C17		123.953
C2	-	129.5128	C15		107.863
C1	-	129.4984	C13		105.600
C4	-	126.911	C6		101.297
C17	-	125.1932	C3		97.372
C5	-	118.5487	C5		95.221
C22	-	114.7369	H18		8.437
C20	-	113.7011	H20		8.095
C27	-	53.6782	H24		7.611
C10	-	18.8263	H9		7.554
C35	-	14.8741	H7		7.361
OH	14.43	13.1312	H8		7.083
CH=N	8.65	8.4847			
Ar-H7	7.12	7.5248			

Ar-H8		7.5130
Ar-H9		7.1718
OCH ₃	4.02	3.5149
C31H ₃	2.44	2.8522
Ar-H17	8.08	7.9194
Ar-H20		7.8158
C35H ₃	2.37	2.6546

3.3 HOMO-LUMO analyse

Chemical events that occur between molecules are typically explained using molecule boundary orbitals. The boundary orbitals in this context are the highest-energy occupied molecular orbital (HOMO) and the lowest-energy empty molecular orbital (LUMO). Because most chemical reactions involve the gain or loss of electrons, HOMO and LUMO have a direct effect on the chemical activity of the molecule. The lower the energy of the lowest energy empty molecular orbital (LUMO) into which the electron to be taken will be inserted, the easier it will be to take the electron. Because electrons are supplied by the highest energy-filled molecular orbital (HOMO), the higher the energy of this orbital, and the more probable it is to donate electrons. The HOMO and LUMO energy values for the compounds employing 6-311++G were calculated using the B3LYP method (d, p). The energy band gap between the ground state and the first excited levels of MMP and FMP compounds exists are around 1.34 eV and 3.64 eV, according to the calculation (Figure 3.2).

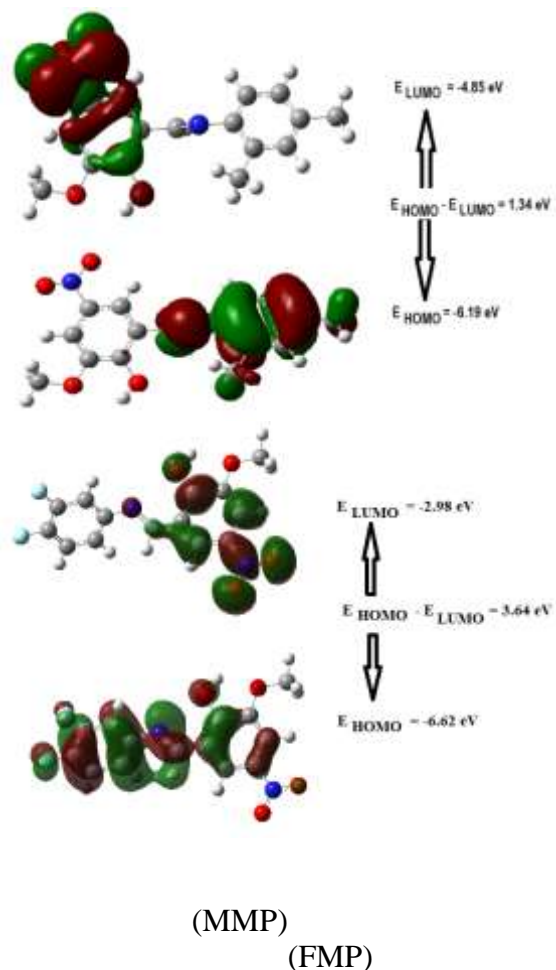


Figure 3.2 The frontier molecular orbitals of MPM and FPM

3.4 Nonlinear Optical (NLO) Properties

Organic materials are important materials for rapid information retrieval and optical storage applications. In organic materials, optical properties are determined by polarizability. The polarizability of an atom or molecule differs from the stable states of the nucleus and electrons. It is a measure of how easily they can

be displaced. The easily displaced electrons in an atom or molecule are the valence electrons, which are farthest from the nucleus. Therefore, valence electrons have a great contribution to polarizability.

It is possible to change or increase the nonlinear optical properties of a molecule. One way to increase the nonlinear optical properties of the molecule is to increase the length of the molecule with conjugated π bonds. Increased conjugation in the molecule leads to an increase in nonlinear optical properties. Another way to increase the nonlinear optical properties is to attach a donor-acceptor group to the ends of the molecules.

Thus, if the delocalization of the π -electron cloud on the molecule increases, the polarizability value of the molecules increases [18,19].

The dipole moment (μ), static polarizability (α_0), and initial static hyperpolarizability (β_{tot}) of structures are all intimately connected to their nonlinear optical (NLO) activity. The polarizabilities and hyperpolarizabilities determined from Gaussian 09 output were translated from atomic units to electrostatic units.

(α : 1a. u = $0.1482 \cdot 10^{-24}$ esu; β : 1a. u = $8.6393 \cdot 10^{-33}$ esu) [20]. The total static dipole moment, μ is defined as shown in Equation (3.1).

$$\mu = (\mu_x^2 + \mu_y^2 + \mu_z^2)^{1/2} \quad (3.1)$$

As given in Equation 4.2 and Equation 4.3, the calculations of static polarizability (α_{ave}) and first static hyperpolarizability (β_{tot}) from the Gaussian output have been stated in detail previously

$$\langle \alpha \rangle = 1/3 (\alpha_{xx} + \alpha_{yy} + \alpha_{zz}) \quad (3.2)$$

$$\beta_{tot} = [(\beta_{xxx} + \beta_{xyy} + \beta_{xzz})^2 + (\beta_{yyy} + \beta_{yzz} + \beta_{yxx})^2 + (\beta_{zzz} + \beta_{zxx} + \beta_{zyy})^2]^{1/2} \quad (3.3)$$

Because of its characteristics in the research of nonlinear optical properties, urea is regarded a generic reference.

The NLO characteristics of the molecules under consideration are assessed by comparing them to urea. Urea values acquired from DFT/B3LYP/6-31G calculations (d), $\mu = 1.3732$ Debye, $\alpha = 3.8312 \text{ \AA}^3$ and $\beta = 0.37289 \cdot 10^{-30} \text{ cm}^5/\text{esu}$ [21]. The computed electric dipole moment, polarizability, and first-order hyperpolarizability properties of the investigated substance are provided in Table 4.7 and Table 4.8. The results show that hyperpolarizability of MMP 78.52 times larger than the urea and hyperpolarizability of FMP 71.08 times larger than the urea. According these results the MMP and FMP compounds presents nonlinear optical activity and these compounds used as nonlinear optical material.

Table 3.1 The electric dipole moment μ (D), the mean polarizability $\langle \alpha \rangle$ and the first hyperpolarizability (β_{tot}) of MMP and FMP compounds by DFT/B3LYP/6-311++G(d,p) level of theory

Parameter	MMP	M P	Parameter	MMP	F M P
μ_x	-0.3285	1.3235	β_{xxx}	-1347.83	2065.45
μ_y	0.3296	1.5021	β_{xyy}	-232.97	-541.58
μ_z	0.5267	-0.5254	β_{xyy}	37.37	616.77
μ_{tot}	0.7028	2.07	β_{yyy}	19.40	-779.70
α_{xx}	419.41	352.88	β_{xxz}	95.49	136.41
α_{xy}	-5.37	-1.42	β_{xyz}	16.04	-62.64
α_{yy}	198.40	212.53	β_{yyz}	29.65	91.17
α_{zz}	-5.65	2.66	β_{zzz}	-3.04	66.44
α_{yz}	0.88	7.73	β_{yzz}	10.19	-28.08

α_{zz}	129.9 0	114. 88	β_{zzz}	42.62	- 45.0 9
$\langle \alpha \rangle$ (a.u)	249.2 3	226. 76	β_{tot} (a.u)	1339.69	3067 .44
$\langle \alpha \rangle$ (esu)	36.93 $\times 10^{-24}$ esu	33.6 1 x 10^{-24} esu	β_{tot} (esu)	11573.9 8×10^{-33} esu	2650 0.5 $\times 10^{-33}$ esu

3.5 Molecular Electrostatic Potential (MEP)

In recent studies in the literature, molecular electrostatics interest in potential (MEP) has greatly increased [22]. The information contained in the MEP is used in different quantum chemical models. MEP is very useful in non-covalent interactions and especially in identifying hydrogen bonds (H bonds). Analysis of 2D or 3D maps of MEP helps to identify sensitive areas in the area around the molecular system that may interact with the proton [23].

3D MEP of MMP and FMP compounds in Figure 4.8 and Figure 4.9 are shown. The MEP shapes of the compounds were obtained as a result of the DFT method and calculations on the B3LYP/6-311++G(d,p) basis set.

In the mentioned 3D MEP surfaces maps, different regions of the molecule are shown with different colors (orange, yellow, green, light blue) in the red-blue range. In the MMP compound of these colors -0.05591 a.u. for red, 0.05591 a.u. for blue found to be worth it. Similarly, in the FMP compound -0.05877 a.u. for red, 0.05877 a.u. for blue found to be worth it. Here, blue color indicates attraction and red color indicates repulsion.

As seen in Figure 4.8 and Figure 4.9, negative potential regions are concentrated near N and O atoms. When we examine the MEP surface map of the compounds in detail, it is remarkable that the blue color is more intense in some regions. These regions are located near the H atoms in the aromatic ring, and near the CH₃ group in the functional group.

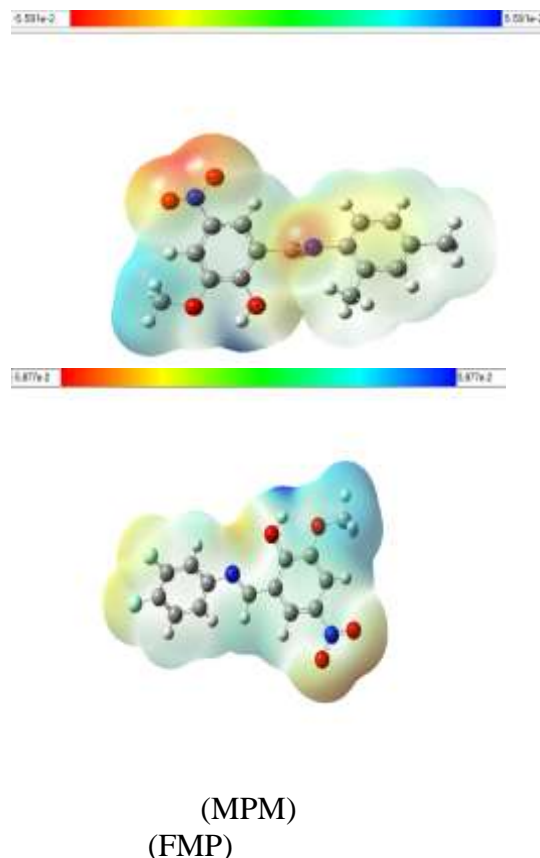


Figure 3.3 Molecular Electrostatic Potential map of MMP and FMP compounds

4 Conclusion

In this study, first of all, geometric optimizations of MMP and FMP molecules were calculated. Experimental and theoretical structural parameters of the mentioned molecules have not been found in the literature. For this reason, experimental values of similar molecules in the literature were found and compared with theoretical values.

In the literature, all C-H bond lengths in the benzene ring have been measured as approximately 1.084 Å, and C-C bond lengths as 1.397 Å. In this study, the aromatic C-H values of MMP compound were calculated as 1.084, 1.085 and 1.086 Å for C3-H7, C4-H8 and C6-H9, respectively. Also, the average value of aromatic C-C bond lengths for MMP compound were calculated as 1.398 Å. In addition, one of the

most important bonds in the studied molecules is the imine bond(C=N). The experimental values of the C=N bond lengths (1E, 2E)-phenyl-[(1-phenylethyl) imino]-ethanal oxime were measured as 1.280 Å and 1.275 Å. Theoretical values were calculated as 1.280 Å and 1.276 Å, respectively.

Vibration spectra and markings were evaluated together experimentally and theoretically. Fundamental vibrations were performed with the GaussView program for marking the vibration spectra. Vibration frequencies were interpreted together with the frequency values of different molecules found in the literature. In the interpretation of frequencies, attention was paid to select the molecules taken as reference from the literature as the closest structure to the molecules studied. ¹H-NMR and ¹³C-NMR values of MPM and FMP compounds were calculated theoretically. Since only the experimental ¹H-NMR values of the MPM molecule were found in the literature, the experimental and theoretical results of this compound were compared. Finally, HOMO-LUMO analysis, non-linear optical properties and MEP surface of the compounds were investigated. It has been observed that the HOMO and LUMO orbitals are generally concentrated in the aromatic ring for the studied molecules. The charge distribution in the molecule was determined by MEP analysis.

References

- [1] Schiff, H. Untersuchungen Uber Salicin Derivate, *European Journal of Organic Chemistry.*, 1869, Vol. 150, 1869, pp.193-200.
- [2] Sharaby, C. M., Amine, M. F., Hamed, A. A., Synthesis, structure characterization and biological activity of selected metal complexes of sulfonamide Schiff base as a primary ligand and some mixed ligand complexes with glycine as a secondary ligand, *Journal of Molecular Structure* Vol. 1134, 2017, pp. 208-216.
- [3] Redshaw, C., Use of Metal Catalysts Bearing Schiff Base Macrocycles for the Ring Opening Polymerization (ROP) of Cyclic Esters, *Catalysts*, Vol.7, No.5, 2017, pp. 165-176.
- [4] Roberts, D. W., Schultz, T. W., Api, A. M., Skin Sensitization QMM for HRIPT NOEL Data: Aldehyde Schiff-Base Domain, *Chemical Research in Toxicology.*, Vol.30, No.6, 2017, pp.1309- 1316.
- [5] Dirisio, R. J., Armstrong J. E., Frank M. A., Lake W. R., McNamara W. R., Cobalt Schiff-base complexes for electrocatalytic hydrogen generation, *Dalton Trans.*, Vol.46, 2017, pp.10418-10425.
- [6] Upadhyay, K. K., Kumar, A., Upadhyay, S., Mishra, P. C., Synthesis, characterization, structural optimization using density functional theory and superoxide ion scavenging activity of some Schiff bases, *Journal of Molecular Structure*, Vol.873, 2008, pp. 5-16.
- [7] Pfeiffer P., Breith E., Lubbe E., Tsumaki T. Tricyclische Orthokondensierte Nebenvolenzringe, *Annalen Der Chemie*, Vol. 503, 1933, pp. 84-127.
- [8] Seçkin T., Köytepe S., Demir S., Özdemir İ., Çetinkaya B., Novel type of metal-containing polyimides for the heck and Suzuki-Miyaura cross-coupling reactions as highly active catalysts”, *Journal of Inorganic Organometallic Polymers.*, Vol.13, No.4, 2003, pp. 223-235.
- [9] Joshi, K. R., Rojivadiya, A. J. and Pandya, J. H., Synthesis and spectroscopic and antimicrobial studies of schiff base metal complexes derived from 2-hydroxy-3-methoxy-5-nitrobenzaldehyde. *International Journal of Inorganic Chemistry*, Vol. 2, 2014, pp. 3-14.
- [10] Frisch, M.J., et al. (2009) Gaussian 09, Revision B. 01. Gaussian, Inc., Wallingford.
- [11] Dennington, R., Keith, T. and Millam, J. 2009. GaussView, Version 5. Semichem Inc. Shawnee Mission KS, 2: 20-30.
- [12] Küçük, İ. 2019. Bazı oksim eter bileşiklerinin sentezi, yapısal, spektroskopik ve fizikokimyasal özelliklerinin deneysel ve kuramsal incelenmesi, Master's thesis, Bursa Teknik Üniversitesi

- [13] Gümüş, H., Fen Bilimleri ve Matematik'te Akademik Araştırmalar. Gece Kitaplığı, 2018, pp. 71-89, Ankara.
- [14] Stuart B. Infrared Spectroscopy: Fundamentals and Applications. Wiley India Ed., 322 p, London, 2010.
- [15] Subashchandrabose, S., Saleem H., Erdogdu, Y., Rajarajanc, G. and Thanikachalam V., FT-Raman, FT-IR spectra and total energy distribution of 3-pentyl-2,6-diphenylpiperidin-4-one: DFT method. *Spectrochimica Acta A: Molecular and Biomolecular Spectroscopy*, Vol.82, 2011, pp. 260-269.
- [16] Ditchfield, R., Molecular Orbital Theory of Magnetic Shielding and Magnetic Susceptibility, *Journal of Chemical Physics*, Vol.56, 1972, pp. 5688–5691.
- [17] Wolinski, K., Hinton J. F. and Pulay P., Efficient implementation of the Gauge independent Atomic orbital method for NMR chemical shift calculations, *Journal of the American Chemical Society*, Vol.112, 1990, pp. 8251–8260.
- [18] Zyss, J., Molecular nonlinear optics: materials, physics and devices, Academic Press, 2013, USA.
- [19] Aggarwal, M. D., Stephens, J., Batra, A. K. and Lal, R. B., Bulk crystal growth and characterization of semiorganic nonlinear optical materials. *Journal of Optoelectronics and Advanced Materials*, Vol.5, No.3, 2003, 555-562.
- [20] Sundaraganesan, N., Kavitha, E., Sebastian, S., Cornard, J.P. and Martel, M., Experimental FT-IR, FT-IR (gas phase), FT-Raman and NMR spectra., Hyperpolarizability studies and DFT calculations of. 3,5-dimethylpyrazole, *Spectrochimica Acta Part A: Molecular and Biomolecular Spectroscopy*, Vol.74, 2020, pp. 788-797.
- [21] Meganathan, C., Sebastian, S., Sivanesan, I., Lee, K. W., Jeong, B. R., Oturak, H., and Sundaraganesan, N. Structural, vibrational (FT-IR and FT-Raman) and UV-Vis spectral analysis of 1-phenyl-3-(1, 2, 3-thiadiazol-5-yl) urea by DFT method. *Spectrochimica Acta Part A: Molecular and Biomolecular Spectroscopy*, Vol. 95, 2012, pp. 331-340.
- [22] Orozco, M. and Luque, F. J. Generalization of the Molecular Electrostatic Potential for the Study of Noncovalent interactions, *Molecular Electrostatic Potentials., Concepts and Applications*, Vol. 2, 1996, pp. 181–218.
- [23] Karabacak, M., Calisir, Z., Kurt, M., Kose, E., Atac, A. The spectroscopic (FTIR, FT-Raman, dispersive Raman and NMR) study of ethyl-6-chloronicotinate molecule by combined density functional theory. *Spectrochimica Acta Part A: Molecular and Biomolecular Spectroscopy*, Vol. 153, 2016, pp.754–770.

Contribution of Individual Authors to the Creation of a Scientific Article (Ghostwriting Policy)

The authors equally contributed in the present research, at all stages from the formulation of the problem to the final findings and solution.

Sources of Funding for Research Presented in a Scientific Article or Scientific Article Itself

No funding was received for conducting this study.

Conflict of Interest

The authors have no conflicts of interest to declare that are relevant to the content of this article.

Creative Commons Attribution License 4.0 (Attribution 4.0 International, CC BY 4.0)

This article is published under the terms of the Creative Commons Attribution License 4.0

https://creativecommons.org/licenses/by/4.0/deed.en_US